CERAMICS

Ultrafast laser welding of ceramics

E. H. Penilla[1], L. F. Devia-Cruz[1,2], A. T. Wieg[1], P. Martinez-Torres[2], N. Cuando-Espitia[2], P. Sellappan[1], Y. Kodera[1], G. Aguilar[2], J. E. Garay[1]*

Welding of ceramics is a key missing component in modern manufacturing. Current methods cannot join ceramics in proximity to temperature-sensitive materials like polymers and electronic components. We introduce an ultrafast pulsed laser welding approach that relies on focusing light on interfaces to ensure an optical interaction volume in ceramics to stimulate nonlinear absorption processes, causing localized melting rather than ablation. The key is the interplay between linear and nonlinear optical properties and laser energy–material coupling. The welded ceramic assemblies hold high vacuum and have shear strengths comparable to metal-to-ceramic diffusion bonds. Laser welding can make ceramics integral components in devices for harsh environments as well as in optoelectronic and/or electronic packages needing visible-radio frequency transparency.

Modern manufacturing is inconceivable without welding, yet reliable ceramic welding is impossible using standard procedures. The same high-temperature resistance that makes engineered ceramics irreplaceable for many demanding applications poses immense obstacles in joining ceramics. This severely limits the complexity of device geometries, confining ceramics to paradigms in which near-net shapes are the only option. Instead of convenient in-atmosphere, room-temperature welding procedures available for metals and polymers, state-of-the art ceramic joining involves high-temperature diffusion bonding. However, diffusion bonding requires long-term exposure of entire assemblies to high temperature and often requires precise modeling of shrinkage dynamics to achieve tight tolerances (*1*, *2*). Thus, reliable diffusion-bonding processes only exist for a limited number of ceramics and are available only for high-cost components.

The joining conundrum is historically one of the biggest impediments to the widespread use of engineered ceramics. The controllable energy deposition offered by lasers is key in additive manufacturing (*3*, *4*) and could be instrumental in efficient ceramic joining. Lasers have been shown to melt ceramics (*5*, *6*); however, attempts to weld ceramics using powerful continuous-wave (CW) lasers without high-temperature preheating have been unsuccessful because of macroscopic cracking attributed to thermal shock (*7*–*9*).

Successful demonstrations of joining glasses were accomplished with ultrafast pulsed (UF) lasers (*10*). Some of the glasses that have been successfully welded (such as borosilicate) have lower fracture toughness and thermal shock resistances than typical engineered ceramics (such as stabilized zirconia and alumina), so thermomechanical properties are not as much of an impediment to laser welding. Instead, the drastically different optical properties, which are due to typical ceramics being translucent to opaque at the laser wavelength instead of transparent like glass, are the crux of the problem. Successful UF laser joining in glasses relies on the ability to focus the laser into the material, stimulating nonlinear and multiphoton absorption processes that lead to localized absorption and melting (*11*). We hypothesized that tuning optical transparency (absorption plus scattering) allows focusing of laser light into the ceramics, placing the energy where it can cause localized melting at the interfaces, effectively welding ceramic components.

To highlight the versatility of this approach, we demonstrate UF laser welding of both transparent ceramics with varying absorption properties and conventionally sintered ceramics that have limited light transparency (scatter or diffuse light). Our strategy considers both the optical properties of the polycrystalline ceramics [linear and nonlinear absorption (NLA)] and laser parameters [exposure time, number of laser pulses, and pulse duration (femtosecond versus picosecond)]. We present two different concepts, transparent ceramics for hermetic encapsulation (concept 1) and diffuse ceramics to demonstrate joining of simple geometries (concept 2).

We show concept 1 using a welded ceramic assembly of a cylindrical cap placed in a tube that can be used for electronic packaging (Fig. 1A) along with a sample payload (Fig. 1B). This configuration takes advantage of the ceramic's transparency to focus the laser at the cap-tube interface while the assembly is rotated, welding the interface. Because the UF laser deposits energy locally, the temperature in most of the assembly is unchanged, which allows temperature-sensitive materials or components such as polymers, metals, or electronic payloads to be encased without damage. We were able to successfully join the cap to the cylinder (Fig. 1C). The ceramic cylinders have outer diameters of 18 mm, and the weld depths are ~1 mm. The backlit background pattern (3.5-mm pitch) is visible through the ceramic cap. Ceramics have inherently lower radio frequency (RF) absorption compared with metals, which, combined with optical transparency, allows for visible-RF light access to electronics and optoelectronic devices through the ceramic package. This is useful for communication as well as wireless electronic charging of optoelectronic devices that can be encapsulated.

Concept 2 mirrors traditional welding of relatively simple geometries. We focused the laser on the interface of two ceramic cylinders from the outside (Fig. 1D). We introduced a small gap so that the ceramics are not in direct contact in order to focus light at the interface of the diffuse ceramics. This ensures limited but adequate optical access to the interface. We successfully welded tubes using this strategy (Fig. 1E). The ceramic tubes have outer diameters of 12 mm and 18 mm, and the weld depths are ~1 mm.

The UF laser joining approach works on two of the most important engineering ceramics, polycrystalline alumina (Al_2O_3) and yttria-stabilized zirconia (YSZ) (Fig. 1E). Alumina and YSZ are extremely versatile ceramics that have useful high-temperature structural properties (*12*–*14*) and widespread electronic applications (*15*, *16*) and are biocompatible (*17*, *18*) so that they can be used in biomedical implants (*19*, *20*). We concentrated on YSZ because optical transparency of YSZ can be tuned by using simple thermal treatments (*21*). The transparency tuning is instrumental in tailoring the laser energy–material coupling. Laser-induced melting occurs under relatively mild average laser powers (<50 W). By operating in this regime, we were able to weld ceramic parts (Fig. 1C) using concept 1, which is capable of holding high vacuum with leak rates satisfying hermetic-quality seal standards for military, space, and bio-implantable electronics (*22*).

We characterized the linear optical absorption and scattering characteristics of the optical-grade YSZ, which are highly dependent on defects and micro- and nanostructure. YSZ has a bandgap (E_g) of 6.1 eV and should be transparent in the visible and near infrared. Most engineered YSZ ceramics are translucent to opaque because the sintering processes used for fabrication lead to relatively high concentrations of residual porosity. Pores efficiently scatter light by introducing a strong refractive index mismatch, Δn, between pores ($n \approx 1$) and matrix ($n \approx 2$). The laser light interacting with traditionally sintered ceramics is strongly scattered by residual porosity, resulting in low optical transparency (Fig. 2, A and B). The high scattering leads to minimal penetration in the material, complicating precise distribution of radiation and potentially resulting in surface evaporation or ablation. The small gap we introduced at the part interfaces facilitated optical penetration, allowing us to circumvent this problem. This strategy is useful for certain simple geometries in which welding occurs at directly accessible interfaces.

Refractive index mismatch that may lead to detrimental scattering is also dependent on the phase composition and grain size. Pure ZrO_2 has a monoclinic structure at room temperature.

[1]Materials Science and Engineering Program and Mechanical and Aerospace Engineering Department, University of California, San Diego, CA, USA. [2]Mechanical Engineering Department, University of California, Riverside, CA, USA.
*Corresponding author. Email: jegaray@ucsd.edu

Yttrium addition stabilizes the tetragonal and cubic structures. The cubic structure is optically isotropic, the tetragonal is uniaxial, and monoclinic is biaxial. The anisotropic optical properties lead to scattering in randomly oriented polycrystalline materials. We can decrease scattering efficiency by producing materials with grain sizes substantially smaller than the wavelength of interest (*23*). We densified transparent YSZ ceramics using current-activated pressure-assisted densification (CAPAD), a process that leads to minimal porosity and fine grains, allowing optical transparency in a variety of ceramics (*24*, *25*)

The YSZ ceramic that we prepared with CAPAD has low laser light scattering but high absorption (Fig. 2C) with a grain size of ~100 nm (Fig. 2D). This permitted us to tightly focus laser light in the material volume rather than diffusively scattering it near the free surface. The optical transparency of YSZ allows for fewer restrictions on the geometry of the welded parts because the light is focused through the ceramic itself. The YSZ is amber colored (Fig. 2D) because of oxygen vacancy–related point defects (*26*). We can decrease the concentration of oxygen vacancy–related defects with longer air annealing (Fig. 2F), changing the transmission in the visible and NIR (Fig. 2G).

The effect of NLA during UF laser–material interaction can be divided into nonthermal (ablation, plasma formation) and thermal effects (melting, evaporation) (*10*, *11*, *27*). At low repetition rates and high energies, nonthermal effects are favored. These effects are used in pulsed-laser deposition of thin films (*28*) and to write useful photonic structures such as waveguides and gratings (*29*). At low energies and high repetition rates, at conditions below the ablation threshold, photonic structures are fabricated by electric field–induced defect migration and/or melting (*30*). Along these lines, we conjectured that by tuning the material's absorption properties to operate in the UF regime at high repetition rates, we could identify a laser processing window leading to highly localized melting in the ceramic interior usable for welding instead of the typically observed ablation.

To evaluate these effects, we conducted Z-scan measurements with a UF laser operating at 1028 nm on the set of annealed samples. Figure 2H plots transmission measurements as a function of Z-scan position, showing decreased transmission at peak intensities, near the focal point at Z = 0 mm. The Z-scan measurements show that the NLA is dominated by two-photon absorption (TPA) (*31*) and is substantially lower in the samples with longer annealing (lower concentration of O vacancy defects). Together, the data in Fig. 2, G and H, show that both the linear and NLA absorption of YSZ can be tuned by simple annealing treatments. The high linear transparency makes it possible to focus deep in the material, similar to glasses, and the large NLA enables efficient laser-material coupling in the beam focus, allowing precise placement of energy at part interfaces that lead to localized melting useful for welding. Because the TPA coefficient is dependent on the peak intensity, it is also likely that laser pulse width in the UF regime (femtosecond versus picosecond pulses) and energy per pulse should influence the resultant material response (melting versus ablation regimes).

We conducted systematic laser-material interaction tests on YSZ to identify the processing windows. We varied the number of laser pulses from 2500 to 250,000 for both the high-absorption and low-absorption samples (Fig. 3A). We identify a radial laser-affected zone (LAZ) emanating from the center of the laser focus with the LAZ diameter clearly growing with the number of pulses. The LAZ for both samples is similar at a low number of pulses (2500 and 5000) but is larger for the high-absorption sample as the number of pulses increases (Fig. 3B).

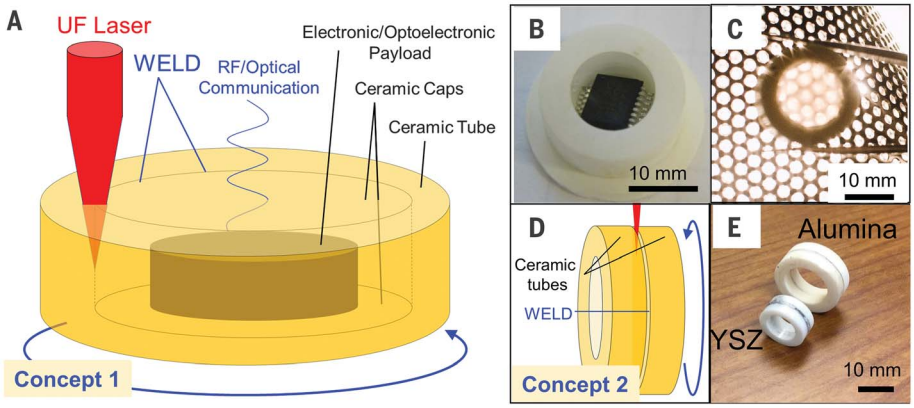

Fig. 1. Two concepts for UF laser welding of ceramics. (**A**) Schematic of concept 1 for ceramic encapsulation. A ceramic assembly (tube + cap) are welded for electronic packaging. The blue arrow indicates rotation axis. RF and/or optical access (depicted with blue curve) is possible through the transparent ceramic cap. (**B**) Picture of a sample electronic payload (an Integrated circuit) placed inside a ceramic tube. (**C**) Picture of successfully welded concept 1 assembly. The background pattern (pitch = 3.5 mm) is visible through a transparent ceramic cap. (**D**) Schematic of concept 2 for welding simple ceramic geometries. (**E**) Picture of successfully welded concept 2 alumina and YSZ assemblies.

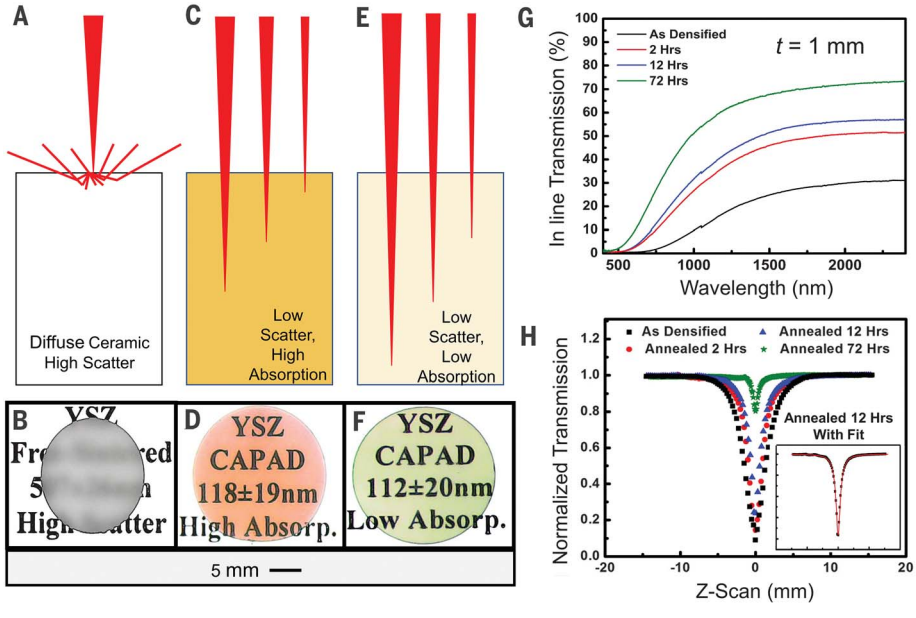

Fig. 2. Tailoring optical properties of YSZ. (**A**) Schematic of a diffuse ceramic that causes significant light scattering. (**B**) Picture of diffuse YSZ. (**C**) Schematic of a ceramic with high absorption and low scatter. (**D**) Picture of a YSZ with high absorption (Absorp.) and low scatter. (**E**) Schematic of a ceramic with low absorption and low scatter. (**F**) Picture of YSZ with low absorption and low scatter. (**G**) Linear transmission measurements of YSZ samples with varying heat treatments (annealing time in air). (**H**) Nonlinear transmission (Z-scan) measurements of YSZ with varying annealing time.

The grains in the LAZ (Fig. 3D) are noticeably larger and elongated compared with the native ceramic, which is evidence of melting because coarsening cannot be explained through diffusional processes at these processing time scales. The native microstructure is similar to that of the transparent (cap) portion (Fig. 1D).

We varied laser pulse length and found that the 2-ps pulses cause a larger diameter than the 230-fs pulses (Fig. 3C). The larger diameter is due to the excited electron cooling, and phonon relaxation occurs on the order of ~1 ps (*32*). We believe this regime is important for successful joining schemes because it sets the temporal pulse width required to produce large melt pools without the deleterious effects of material removal. Investigations of laser pulses on ceramics tend to focus on the femtosecond regime rather than the ps regime. Thermalization, the energy transfer to the lattice from the hot electron gas, does occur under femtosecond excitation, but the high peak intensities along with rapid arrival of successive pulses tends to further increase the electron gas temperature. This leads to plasma formation and material removal (*32*).

Considerably higher power is necessary for melting ceramics when using CW lasers instead of UF lasers. For example, Li *et al.* used a 200-W CW laser to induce melting for a ceramic additive manufacturing process (*33*). Similarly, Fantozzi *et al.* used a 200-W CO_2 laser to weld mullite to glass (*7*, *8*), and Exner (*8*) used a 1.2-kW Nd doped yttrium-aluminum-garnet (Nd:YAG) laser to weld alumina ceramics. In these studies, the poor optical transparency (high scatter) of traditional ceramics along with relatively slow heating associated with linear absorption results in an unfavorable heat-affected zone with most of the laser energy being delivered near free surfaces, resulting in high thermal gradients and cracking. The use of halogen lamps and secondary lasers to preheat and post cool the ceramic parts along with primary lasers to melt the joints without causing severe thermal gradients overcomes these problems. Whereas this approach is effective for some niche joining procedures, traditional diffusion bonding is still the preferred strategy because the global part temperatures for the CW methods are >1600°C, which is similar to the furnace temperature used in diffusion bonding. By contrast, our strategy creates localized melting with substantially lower laser powers, which is possible because the low scatter and linear absorption permit tight focusing of the laser into the ceramic. When the light is delivered as UF pulses, it results in a spatially confined NLA due to high TPA.

We measured the melt diameter with the number of laser pulses. Our samples initially show a relatively linear LAZ diameter increase followed by a plateau-like behavior as pulse numbers increase. Increasing pulse energy also leads to a larger LAZ diameter at a given pulse number. The low-absorption samples plateau at a lower number of pulses compared with high-absorption samples. The linear regions (Fig. 3, B and C) are the UF laser processing windows we determined empirically in which increasing the number of pulses leads to an increased melt diameter useful for ceramic welding. As the number of pulses increases, the melt diameter plateaus as ablation begins to dominate over melting.

We found the effective processing window is larger for picosecond compared with femtosecond and for higher-absorption samples. Thus, a relatively low number of pulses and pulse lengths in the picosecond regime results in good energy coupling at a 1-MHz repetition rate. A successful weld requires not only melting at a point but also continuous melting along the joint interface. We accomplished this by dynamically rotating the ceramics through the beam focus at corresponding angular velocities while holding the pulse energy and repetition rate constant (Fig. 4A). This ensures that an ideal number of incident pulses impinge on an area as guided by the static LAZ diameters obtained at a specific energy and pulse width, resulting in a continuous weld pool at the mating surfaces. An example weld using this strategy was made on diffuse alumina (Fig. 3E). We found clear signs of melting with stark differences in microstructure and the presence of dendritic structures in the LAZ.

We rotated ceramic interfaces at varying angular speeds of 30, 50, and 80° s^{-1}, using concept 1 corresponding to equivalent pulse doses of ~100,000, 50,000, and 25,000 (Fig. 4B). Because the parts we joined ranged from 12.5 to

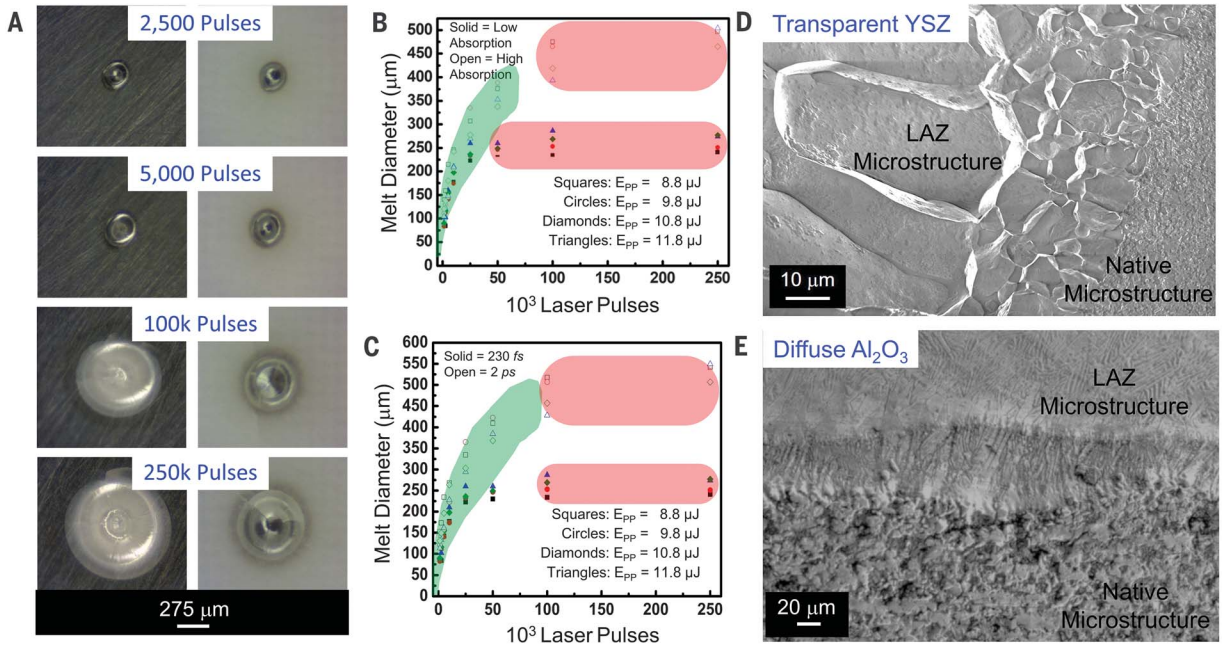

Fig. 3. Pulsed laser–material interactions. (**A**) Optical micrographs of YSZ subjected to varying number of UF laser pulses, high-absorption sample (left), and low-absorption samples (right). (**B**) Effect of number of laser pulses on resulting melt diameter for samples with low and high absorption. (**C**) Effect of number of laser pulses on resulting melt diameter for 2-ps and 230-fs pulse widths. The green-shaded regions denote efficient energy coupling; in the red-shaded areas, increasing pulses do not increase melt diameter (poor energy coupling). (**D**) SEM micrographs of cross section of YSZ near LAZ. The microstructure reveals elongated grains in LAZ and isotropic grains in the native microstructure. (**E**) SEM micrographs of cross section of alumina near LAZ. The microstructure reveals dendritic in LAZ and isotropic grains in the native microstructure.

19 mm in diameter, the weld speeds were 3.3 to 13.1 mm s^{-1}, and total time for welding procedure was ~2 to 20 s. The parts we processed at the lowest angular speed showed signs of ablation, so the welds were not successful. The failed welds were in line with our interaction tests (Fig. 3), as high numbers of laser pulses lead to ablation. The interface we rotated at an angular speed of 50° s^{-1} shows signs of melting and has an optimal weld bead reminiscent of some metal welds (Fig. 4C). We also found melting at the highest angular speed, but the melted volume was not uniform (Fig. 4D).

We observed a similar dependence of weld quality on processing parameters in the diffuse ceramic case. We achieved light penetration in the concept 2 welds by introducing a small gap of approximately half the width of the full width at the half maximum (FWHM) of the focused laser beam while rotating the ceramic tubes through the laser focus as shown in Fig. 1D. For our welds, this gap is ~12.5 μm between the interfaces of the optically diffuse ceramic parts. Our attempts to produce welds for parts in physical contact resulted in poor interaction volumes dominated by ablation and material removal near the free surfaces. When we increased the gap dimension beyond half of the FWHM of the focused laser beam, we required increased laser powers to induce sufficient laser-material coupling. We also found that the interaction zones did not correlate to the laser interaction tests on flat surfaces, because the effective pulse profile interacting with the ceramics was substantially different.

To test the efficacy of the concept 1 welded YSZ encapsulation tube and cap, we subjected the welded ceramic assembly to vacuum testing (Fig. 4E). The welded assembly was placed in vacuum fixtures supported by polymer O-rings such that the welded regions were exposed to atmosphere on one side and a high vacuum on the other (*31*). We chose this design to simulate a welded capsule or package used to encase temperature-sensitive components (Fig. 1, A and B). The assembly holds a high vacuum, with an ultimate pressure of 3.2×10^{-7} mbar. We measured a leak rate of 1.29×10^{-7} mbar cm^3 s^{-1} for the welded ceramic vessel (Fig. 4F), approximately one order of magnitude better than the requirement for hermetic-quality seals. Our assembly satisfies modern specifications and standards (Mil-STD-883 TM 1014.12) for encapsulating military, space, and bio-implantable electronics (*22*). For comparison, we also vacuum-tested a poorly welded vessel and found that the leak rate was four orders of magnitude higher (Fig. 4F, inset). We could not attain vacuum-level pressures when testing assemblies that were in mechanical contact but not welded.

We used mechanical testing to assess the quality of concept 2 welded assemblies. We tested the shear strength of free sintered YSZ tubes joined together (Fig. 1D) using a shear testing fixture (Fig. 4H) (*31*). Our tests show that the strength of the welds varies with laser processing parameters (Fig. 4H). The cylinders joined by using femtosecond pulse lengths and intermediate (50° s^{-1}) speeds have the lowest shear strength around 7 MPa. The low speeds (30° s^{-1}) using picosecond pulses have an average of 17 Mpa, and the intermediate speed using picosecond pulses yield shear strengths of ~40 MPa. Strengths close to the inherent bending strength of ceramics have been obtained for ceramic-ceramic diffusion bonding at high temperatures (for example, 1500°C) and long hold times, on order of 10 hours (*1*). Diffusion-bonding temperatures can be decreased by using metal layers. For example, Travessa *et al.* report alumina diffusion bonding to stainless steel using Ti layers with shear strengths ranging from 23 MPa and using

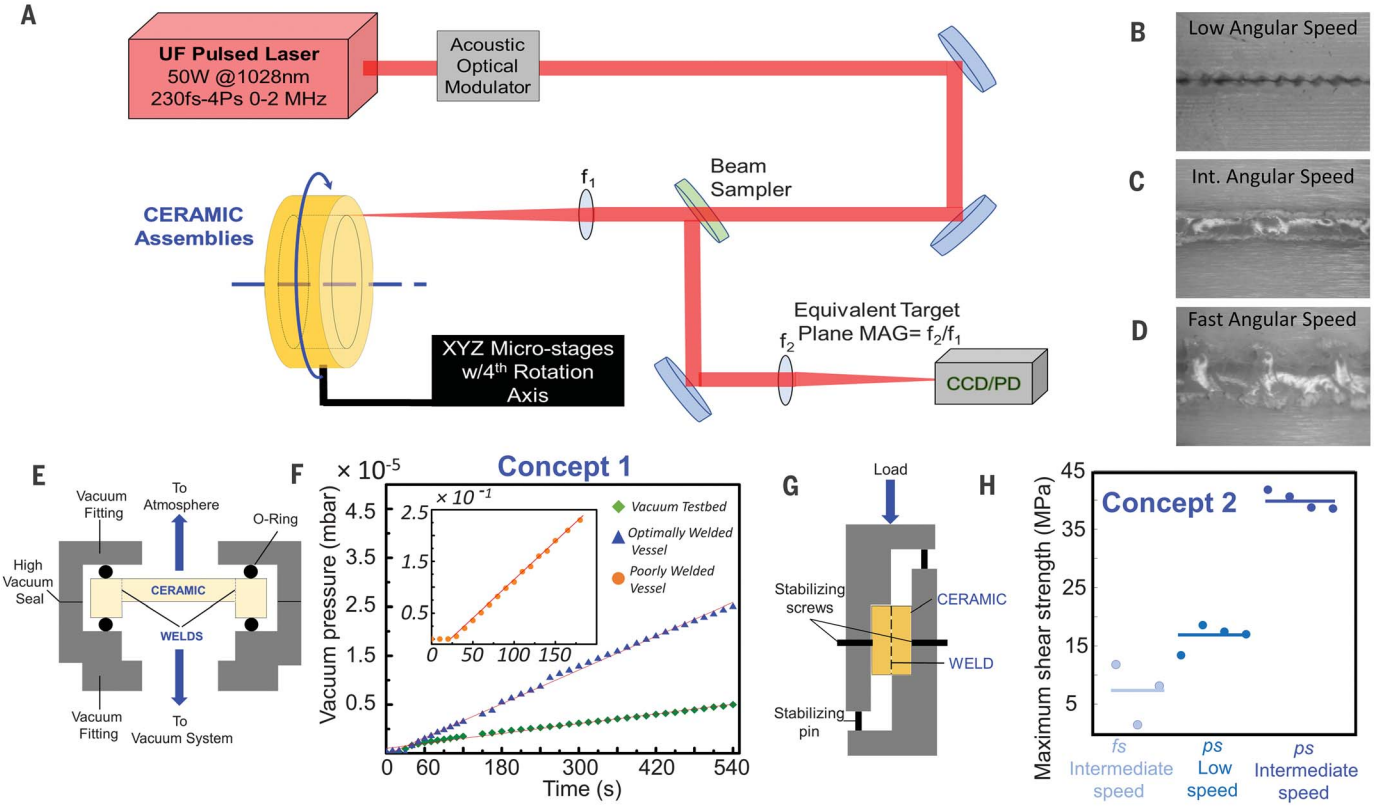

Fig. 4. Laser welding of YSZ ceramic assemblies. (**A**) Schematic of laser welding rig. The UF laser is focused on interfaces and the assembly is rotated, creating a welded seal. CCD, charge-coupled device; MAG, Magnification; PD, Photodiode. (**B** to **D**) Optical micrograph of weld created with a low angular rotation velocity (B), intermediate (Int.) angular rotation velocity (C), and high angular rotation velocity (D). (**E**) Schematic of vacuum leak test bed for laser-welded concept 1 assembly. (**F**) Vacuum pressure versus time test results (leak-rate measurements). (**G**) Schematic of rig used for testing leak rate of laser-welded assembly. (**H**) Shear test results for concept 2 assemblies joined using different laser parameters. The points represent individual tests, and the line is the average of the tests.

~65 MPa using Cu layers (*34*). Thus, the highest shear strengths obtained in this study are comparable to joints obtained using diffusion bonding of ceramics to metals. Those ceramic-metal diffusion bonds were accomplished at global part temperatures ranging from 700 to 900°C, whereas the ceramic assemblies reported with our technique were joined at room temperature. The strength of laser welds could vary with sample size because some observations of ceramic strength show it decreases with increasing sample size. However, welded joints on ceramics with dimensions and strengths that we obtained will be useful for a variety of current applications.

We can compare the energy efficiency of the UF laser welding with traditional diffusion bonding by considering energy consumption in the processes. A high-temperature furnace typically consumes ~1000 W, and with ~5 hours of bonding time, the energy consumption is ~5000 W·hour. The UF laser used in this study has a maximum power of 50 W, and assuming an optical power conversion efficiency of 10%, the short welding times allow for an energy consumption on the order of 25 W·hour. We have not optimized these joints for strength, and it is highly likely that the strength can be raised substantially. Possible optimization strategies for improved welds include more tailored gap distance, improved focal length, different surface treatments, and an NLA changed with impurities or thermal treatments.

UF laser welding is more versatile on transparent ceramics because one can focus through the material, allowing the joining of more complex geometries and over multiple interaction zones, increasing the ultimate weld volumes. Our strategy should be applicable to a wide range of other oxides, nitrides, and carbides. This includes the array of available transparent ceramics with similar optical bandgaps, including alumina (*35*), spinel (*36*), YAG (*37*), and many others under development (*38*–*40*). Ultrafast lasers with different wavelengths and suitable laser powers likely will become more widely available, expanding the potential usefulness of our technique. The absorption properties required for welding other ceramics are determined by the electronic structure and defects, requiring additional wavelength tuning or the engineering of absorption using intrinsic point-defect complexes such as anion or cation vacancies or dopants like transition metal or rare earths. Our welding concepts should be helpful for producing ceramic micromechanical systems, lab-on-a-chip devices, and biocompatible or chemical- and temperature-resistant electronic and optoelectronic packaging. The visible-RF light access allowed by ceramic packaging is important for developing optoelectronic devices, facilitating optical communication as well as wireless electronic charging.

REFERENCES AND NOTES

1. J. A. Fernie, R. A. L. Drew, K. M. Knowles, *Int. Mater. Rev.* **54**, 283–331 (2009).
2. O. K. Akselsen, *J. Mater. Sci.* **27**, 569–579 (1992).
3. Z. C. Eckel *et al*., *Science* **351**, 58–62 (2016).
4. J. H. Martin *et al*., *Nature* **549**, 365–369 (2017).
5. I. Shishkovsky, I. Yadroitsev, P. Bertrand, I. Smurov, *Appl. Surf. Sci.* **254**, 966–970 (2007).
6. C. Y. Yap *et al*., *Appl. Phys. Rev.* **2**, 041101 (2015).
7. C. Riviere, M. Robin, G. Fantozzi, *J. Phys. IV Colloq.* **4**, 135–138 (1994).
8. A. De Paris, M. Robin, G. Fantozzi, *J. Phys. IV Colloq.* **1**, 127–129 (1991).
9. H. Exner, A.-M. Nagel, in *Proc. of SPIE Laser Applications in Microelectronic and Optoelectronic Manufacturing IV* (SPIE, 1999), pp. 262–268.
10. M. Malinauskas *et al*., *Light Sci. Appl.* **5**, e16133 (2016).
11. K. Itoh, W. Watanabe, S. Nolte, C. B. Schaffer, *MRS Bull.* **31**, 620–625 (2006).
12. N. P. Padture, M. Gell, E. H. Jordan, *Science* **296**, 280–284 (2002).
13. C. L. Hardin, Y. Kodera, S. A. Basun, D. R. Evans, J. E. Garay, *Opt. Mater. Express* **3**, 893 (2013).
14. J. P. Buban *et al*., *Science* **311**, 212–215 (2006).
15. B. C. H. Steele, Material science and engineering: The enabling technology for the commercialisation of fuel cell systems. *J. Mater. Sci.* **36**, 1053–1068 (2001).
16. M. G. Kim, M. G. Kanatzidis, A. Facchetti, T. J. Marks, *Nat. Mater.* **10**, 382–388 (2011).
17. Y. Damestani *et al*., *Biol. Med. (Aligarh)* **9**, 1135–1138 (2013).
18. P. S. Christel, *Clin. Orthop. Relat. Res.* 282, 8 (1992).
19. J. Chevalier, L. Gremillard, S. Deville, *Annu. Rev. Mater. Res.* **37**, 1–32 (2007).
20. M. I. Gutierrez *et al*., *Adv. Healthc. Mater.* **2017**, (2017).
21. S. R. Casolco, J. Xu, J. E. Garay, *Scr. Mater.* **58**, 516–519 (2008).
22. U.S. Department of Defense (DOD), Military specification MIL-883 TM 1014.12, Test methods for semiconductor devices. (DOD, 2004).
23. E. H. Penilla *et al*., *J. Appl. Phys.* **119**, 023106 (2016).
24. J. E. Garay, *Annu. Rev. Mater. Res.* **40**, 445–468 (2010).
25. Y. Kodera, C. L. Hardin, J. E. Garay, *Scr. Mater.* **69**, 149–154 (2013).
26. J. E. Alaniz, F. G. Perez-Gutierrez, G. Aguilar, J. E. Garay, *Opt. Mater.* **32**, 62–68 (2009).
27. T. Tamaki, W. Watanabe, J. Nishii, K. Itoh, *Jpn. J. Appl. Phys.* **44**, L687–L689 (2005).
28. P. Sellappan, C. Tang, J. Shi, J. E. Garay, *Mater. Res. Lett.* **5**, 41–47 (2017).
29. F. Chen, J. R. V. de Aldana, *Laser Photonics Rev.* **8**, 251–275 (2014).
30. G. R. Castillo-Vega, E. H. Penilla, S. Camacho-López, G. Aguilar, J. E. Garay, *Opt. Mater. Express* **2**, 1416 (2012).
31. Materials and methods are available as supplementary materials.
32. A. Hu, Y. Zhou, W. W. Duley, *Open Surf. Sci. J.* **3**, 42–49 (2011).
33. Y. Li, Y. Hu, W. Cong, L. Zhi, Z. Guo, *Ceram. Int.* **43**, 7768–7775 (2017).
34. D. Travessa, M. Ferrante, G. Den Ouden, *Mater. Sci. Eng. A* **337**, 287–296 (2002).
35. E. H. Penilla *et al*., *Light Sci. Appl.* **7**, 33 (2018).
36. M. Rubat du Merac, H. J. Kleebe, M. M. Müller, I. E. Reimanis, *J. Am. Ceram. Soc.* **96**, 3341–3365 (2013).
37. S. H. Lee *et al*., *J. Am. Ceram. Soc.* **89**, 1945–1950 (2006).
38. A. Ikesue, Y. L. Aung, *Nat. Photonics* **2**, 721–727 (2008).
39. A. D. Dupuy, Y. Kodera, J. E. Garay, *Adv. Mater.* **28**, 7970–7977 (2016).
40. A. T. Wieg, E. H. Penilla, C. L. Hardin, Y. Kodera, J. E. Garay, *APL Mater.* **4**, 126105 (2016).

ACKNOWLEDGMENTS

The authors gratefully acknowledge M. Duarte for assistance with optical microscopy, A. Zhao for help with preparing photographs used in the figures, and F. Angeles for assistance in preparation of diffuse ceramic samples used for welding studies. We also thank V. Lubarda for helpful discussions. **Funding:** Funding of this work by Defense Advanced Research Projects Agency (DARPA contract HR0011-16-2-0018) is most gratefully acknowledged. Partial funding from the Office of Naval Research (ONR-N00014-17-1-2594) is also gratefully acknowledged. The National Science Foundation (NSF-PIRE grant contract 1545852) and UCR's Office of Research and Economic Development are also acknowledged for the financial support toward the purchase of the laser system. **Author contributions:** E.H.P, A.T.W., and Y.K. synthesized, processed and performed post processing of materials. E.H.P., P.S., and Y.K. performed and contributed to material structural and microstructural characterization. E.H.P. and P.M.-T. performed linear and nonlinear optical characterization. E.H.P. and L.F.D.-C. designed and performed static laser-material interaction experiments and laser welding experiments with guidance from G.A. and J.E.G.; N.C.-E. performed thermal analysis with guidance from G.A. and J.E.G.; E.H.P. designed and performed vacuum leak rate testing with guidance from J.E.G.; E.H.P., L.F.D.-C., and A.T.W. contributed to and performed mechanical tests. G.A. and J.E.G. conceived of laser welding and electronic packaging concepts. E.H.P. and J.E.G. analyzed results and wrote the manuscript. **Competing interests:** G.A., J.E.G., and E.H.P. have filed a provisional patent application (U.S. Prov. App. 62-879,253) on the work described here. **Data and materials availability:** All data are available in the manuscript or in the supplementary material.

SUPPLEMENTARY MATERIALS

science.sciencemag.org/content/365/6455/803/suppl/DC1
Materials and Methods

14 January 2019; resubmitted 9 May 2019
Accepted 29 July 2019
10.1126/science.aaw6699

Ultrafast laser welding of ceramics

E. H. Penilla, L. F. Devia-Cruz, A. T. Wieg, P. Martinez-Torres, N. Cuando-Espitia, P. Sellappan, Y. Kodera, G. Aguilar and J. E. Garay

Science **365** (6455), 803-808.
DOI: 10.1126/science.aaw6699

Joining the laser welding club

Laser welding is an integral part of modern manufacturing, but it fractures ceramic materials. Penilla *et al.* developed two methods for welding ceramics using ultrafast lasers. One method tunes the ceramic properties, allowing the laser to transit through the ceramic and weld at the interface between pieces. The other method optimizes a gap between pieces to efficiently deposit energy. Both methods leverage short but energetic pulses to create a melt pool that allows ceramics to be joined, without the high temperature used for traditional ceramic welds.

Science, this issue p. 803